

Towards Automatic Construction of Cell-Lineage of *C. elegans* from Nomarski DIC Microscope Images

Tomohiro Yasuda¹² Hideo Bannai¹² Shuichi Onami¹
tyasuda@ims.u-tokyo.ac.jp bannai@ims.u-tokyo.ac.jp sonami@symbio.jst.go.jp
Satoru Miyano¹³ Hiroaki Kitano¹⁴
miyano@ims.u-tokyo.ac.jp kitano@symbio.jst.go.jp

¹ Kitano Symbiotic Systems Project, ERATO, JST M-31 Suite 6A, 6-31-15 Jingumae, Shibuya-ku, Tokyo 150-0001, Japan

² Department of Information Science, Faculty of Science, University of Tokyo, 7-3-1 Hongo, Bunkyo-ku, Tokyo 113-8654, Japan

³ Human Genome Center, Institute of Medical Science, University of Tokyo, 4-6-1 Shirokanedai, Minato-ku, Tokyo 108-8639, Japan

⁴ Sony Computer Science Laboratory, 3-14-13 Higashi-Gotanda, Shinagawa, Tokyo 141-0022, Japan

Abstract

This study aims at automatic construction of a cell lineage from 4D(multi-focal, time-lapse) images, which are taken using a Nomarski DIC (differential-interference contrast) microscope. A system with such abilities would be a powerful tool for studying embryo genesis and gene function based on mutants, whose cell lineage may differ from that of wild types. We have designed and implemented a system for this purpose, and examined its ability through computational experiments. The procedure of our system consists of two parts: (1) Image processing which detect the positions of the nuclei from each 2D microscope image, and (2) Constructing a hypothetical cell lineage based on the information obtained in (1). We have also developed a tool which allows a human expert to easily filter out erroneous nuclei candidates generated in (1). We present computational results and also discuss other ideas which may improve the performance of our system.

1 Introduction

The development of a multi-cellular organism starts from a single cell. This cell divides into two cells, and each of them again divides into two, and so on. The whole relationship of parent cells and their daughter cells is called the *cell lineage*, which can be described as a tree structure. The analysis of the cell lineage is important for understanding the development of multi-cellular organisms [8]. When certain genes are disrupted, the cell lineage may change. Very useful information about the gene function can be obtained, by examining how the cell lineage of mutants changes compared to that of wild types [1, 2]. The main objective we focus on is this gene function analysis.

By using a 4D microscope system, we can record images of an embryo at multiple focal planes and multiple time-points. A human expert can then construct the cell lineage by viewing these images later on. However, when done by hand, such work is very time consuming, and requires extraordinary human effort. A method which automates this procedure will greatly increase the productivity of cell lineage construction. This will allow the systematization of mutant analysis - one of the major projects of post-genome sequencing - from the enormous number of mutants that are emerging from gene-knockout projects.

In this paper, we describe a system which constructs a hypothetical cell lineage automatically from a Nomarski DIC 4D image. We use the Nomarski DIC microscope [7] for two reasons. Firstly, there is no need to dye the organism. This is an important factor because otherwise, there is danger of damaging the genes of the organism, which will give us false data. Secondly, a Nomarski DIC

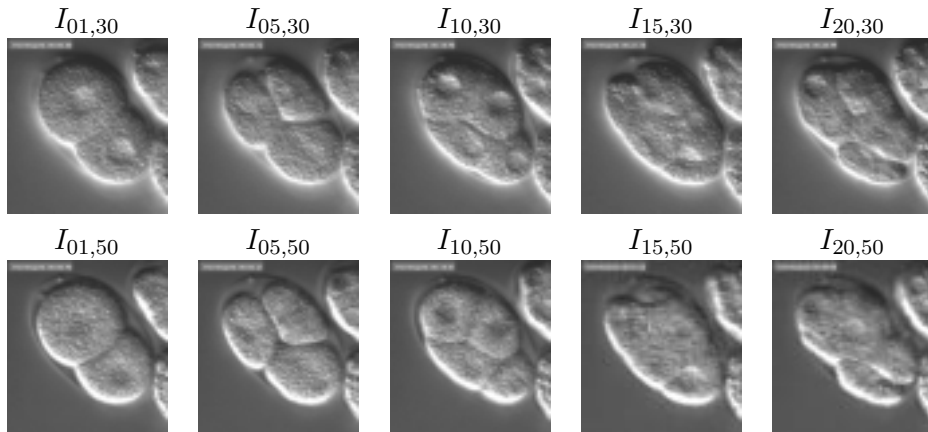


Figure 1: Part of the data set. Images from the 30th and 50th focal planes, at 1st,5th,10th,15th,20th time-points. The notation ‘ $I_{t,f}$ ’ means the image at time-point t and at focal plane f .

microscopes are less expensive compared to a confocal microscope. The development of this technology will contribute to a broader society of scientists.

With a combination of image processing algorithms with certain parameters, the system extracts the positions of the candidate nuclei, as well as the time-points of their emergence and disappearance. The result is then used to construct a hypothetical cell lineage. Although our final goal is to create a system which requires no human intervention, many false positives were created through the nuclei detection process. This interfered with the accurate construction of the cell lineage. Therefore, we have also created a tool that enables a human expert to filter out these false positives with very little effort. We had an expert evaluate this tool, and we note that he was amazed at the ease of this task.

We explain the data set we used in Section 2. In Section 3, we present the details of our system. The results of our experiments are given in Section 4. Finally, we discuss several promising possibilities for the improvement of our system in Section 5.

2 Materials

The data set we used contains Nomarski DIC microscope images of *Caenorhabditis elegans* (*C.elegans*) embryo, from 2-cell stage to 7-cell stage. The size of each image is 299×327 pixels, and the depth of each pixel is 8 bits.

The images were taken at 89 different focal planes at 20 time-points, which amount to 1780 images. The size of the embryo is about $60 \mu\text{m}$ along the longer axis, $30 \mu\text{m}$ along the shorter axis. The interval between two time-points is 90 seconds. Fig. 1 shows some part of the data set.

3 Method

The outline of our cell lineage construction system is presented in Fig. 2.

In order to construct a cell lineage, it is necessary to obtain the information that describes when and where each nucleus emerges and disappears in the images. We developed an image processing algorithm which extracts nuclei from the 2D images one by one. We also implemented an algorithm that integrates the same nucleus detected in different images into a single data structure. With these nucleic information obtained, our system constructs a hypothetical cell lineage.

The following sections describe the algorithm in detail.

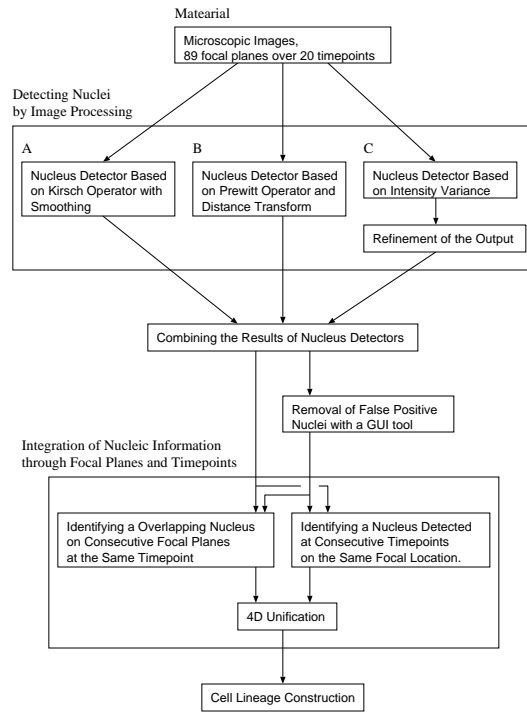


Figure 2: The Outline of Lineage Construction System.

3.1 Detecting Nuclei by Image Processing

We developed three nucleus detectors. Two of them assume that nuclei appear as even regions in the images, each employing a different method to find these regions. The third detector assumes that the intensity of the image changes around a nucleus. The three detectors each look for different characteristics in the image, detecting nuclei with different appearance.

We briefly describe each nucleus detector in the following sections.

3.1.1 Nucleus Detector Based on Kirsch operator with Smoothing.

This nucleus detector captures even regions in the image as nuclei with the Kirsch operator [4] and smoothing. In the microscope images, a nucleus seems rather “flat” compared to cytoplasm filled with organelles, which appears “bumpy”.

The steeper the gradient at the pixel, the stronger the output of the Kirsch operator at the pixel. The Kirsch operator, however, responds also to small local gradient which should be discarded. Therefore, we also employed a smoothing operator, which erases, from the output of Kirsch operator, small bright regions in nuclei and small dark regions in cytoplasm. To emphasize the difference between nucleus area and cytoplasm area, our system also performs the histogram equalization [9].

In the rest of this paper, we refer to this nucleus detector as “Detector A”. The output of the Detector A is binarized into an image, where the nuclei appears as a black region isolated from white cytoplasm (Fig. 3).

3.1.2 Nucleus Detector Based on Prewitt Operator and Distance Transform

We have developed another detector which also captures nuclei as even regions in the image, by using the Prewitt [5] operator and the distance transform [3]. To differentiate the nucleus from the cytoplasm area, we used the distance transform. The binarized output of the Prewitt operator is an image where

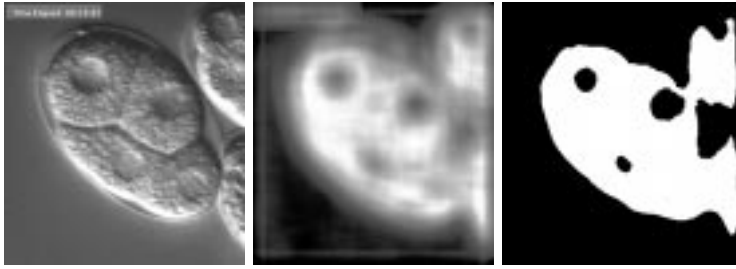


Figure 3: Detector A. From left to right: input, output, and the binarized image.

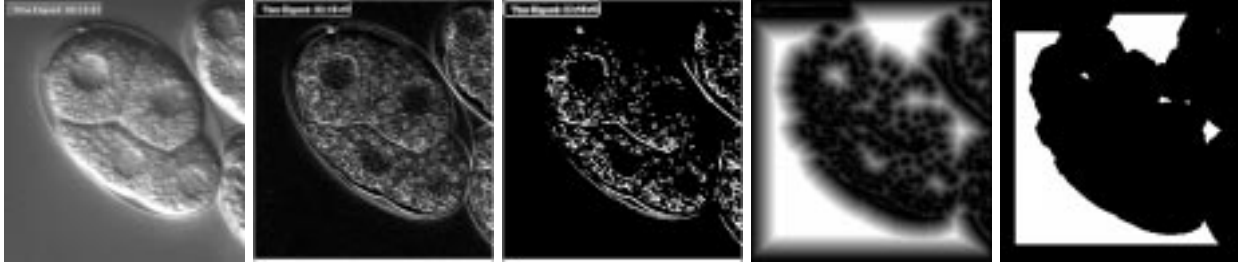


Figure 4: Detector B. From left to right: input, output of Prewitt operator, binarized image, output of distance transform, and the binarized image.

nuclei appear as large black regions and the cytoplasm area has a lot of white dots. The distance transform is then applied to this image, choosing white pixels as the background. Since the center of a nucleus region is relatively far from white pixels in the cytoplasm area, a nucleus appears as a bright region in the output of the distance transform.

Two standard definitions of distance between two pixels, say, (x_1, y_1) and (x_2, y_2) , employed by the distance transform are the *city block distance* [3] and the *chess-board distance* [3].

We modified the chess-board distance as below to approximate Euclidean Distance.

$$d = \begin{cases} 1.5 \times |x_1 - x_2| + (|y_1 - y_2| - |x_1 - x_2|) & \text{for } |x_1 - x_2| \leq |y_1 - y_2| \\ 1.5 \times |y_1 - y_2| + (|x_1 - x_2| - |y_1 - y_2|) & \text{for } |x_1 - x_2| \geq |y_1 - y_2| \end{cases} \quad (1)$$

We also modified the algorithm which calculates the distance transform with the chess-board distance so that the distance transform with our definition of distance can be calculated efficiently (in $O(n)$ time, where n is the number of all pixels in each microscope images).

In the rest of this paper, we refer to this nucleus detector as “Detector B”. The output of this filter is also binarized and analyzed as Detector A.

3.1.3 Nucleus Detector Base on Intensity Variance

The third nucleus detector captures the regions where the intensity of the image changes drastically along a certain direction. As shown in Fig. 1, many nuclei have bright upper rims and dark lower rims. Suppose that we are focusing on a pixel (x, y) of an image. Looking along the supposed direction of light ¹, let the sum of the intensity of pixels of the upper region of (x, y) be S_u , and similarly for the lower region, S_l . If the pixel is inside a nucleus, the absolute value of $S_u - S_l$ should be large.

¹In fact, this is the direction along which two perpendicularly oscillating beams of Nomarski DIC microscope are sheared [7].

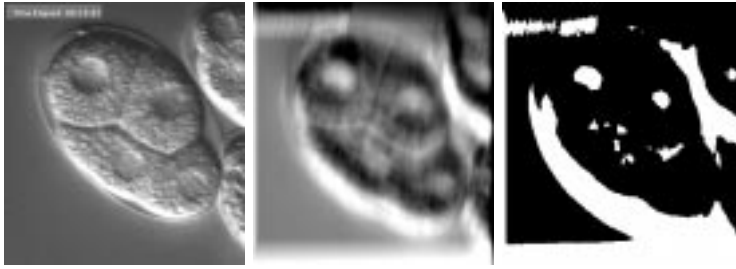


Figure 5: Detector C. From left to right: input, output, and the binarized image. Two upper nuclei were detected successfully, although the remaining two were not.

Here we give a more formal description of this nucleus detector by a mathematical equation. Let $f(x, y)$ be the intensity of the original image, and $g(x, y)$ be the intensity of the output image of this algorithm. This algorithm of Detector C is as follows:

$$g(x, y) = \frac{1}{2m} \left(- \sum_{k=-m}^{-1} f(x + k \cos \theta, y - k \sin \theta) + \sum_{k=1}^m f(x + k \cos \theta, y - k \sin \theta) \right) \quad (2)$$

where θ is the direction to look along, and m is the range to sum up the intensity (Fig. 5).

In the rest of this paper, we refer to this nucleus detector as “Detector C”. The output of this filter is also binarized and analyzed as Detector A and Detector B.

Refinement of Detector C Detector C tends to make many false positives (regions which are falsely detected as nuclei). The false positives have a tendency to appear on:

- the boundary between two cells, and
- the rim of the embryo.

We developed two image processing algorithms which roughly detect the boundary and the area occupied by the egg (let us call this area the *egg-area*) in the image.

The boundary detector employs the Prewitt operator and binarizes the output. Long and narrow regions which have i) appropriately large covering area, ii) appropriate outline length, and iii) low roundness, are recognized as a boundary. We discard a region detected by Detector C if it intersects with one of the regions detected by the boundary detector.

The egg-area detector employs the Kirsch operator. The Kirsch operator is applied to the original image and the output is binarized. Minute white pixels are removed by using the median filter. We assume that the outline of the largest connected component in this binarized image is the outline of the egg-area. We discard a region detected by Detector C if it is not included in the egg-area.

3.1.4 Detecting Nuclei from a Filtered Image

Each of the three nucleus detectors creates an image where the nuclei appear as a bright or dark region. Whether a nucleus appears bright or dark depends on the type and parameters of the detector used. We assume that a nucleus appears as a bright region. (We can always take the complement of an image.)

An output of the detectors is binarized with an appropriate threshold that depends on the type of the detector. Then the nuclei appear as white regions, although there are also lots of white regions which are not nuclei.



Figure 6: A screen shot of *rmfalse*. *Rmfalse* is a tool for removing false positive candidate nuclei.

To pick up only the correct nuclei among white regions, knowledge about the shape of the nuclei was utilized. Our system chooses, as candidate nuclei, regions which i) cover appropriately large area, ii) have appropriate outline length, and iii) have appropriate *roundness* [9].

3.1.5 Integrating the Output of Three Detectors

The outputs of the three detectors have to be combined into one. Roughly speaking, any nucleus detected by at least one of the three nucleus detectors is adopted as a nucleus detected by the whole system. The same nucleus detected by more than two nucleus detectors is joined into a single nucleus.

3.2 Removal of False Positive Nuclei by Human Expert with a GUI Tool

We intend to utilize our cell lineage construction system for biological applications, especially systematic mutant analysis.

Our system at the current state of this project, however, cannot construct a reliable hypothetical cell lineage if we stick to fully automatic lineage construction system. This is mainly because our nucleus detector creates a number of false positive nuclei. We are now trying to improve the nucleus detector and to develop more robust lineage construction algorithm, but it is not an easy task.

To overcome this situation as soon as possible, we developed a GUI tool (Fig. 6) with which a human expert can remove false positive nuclei. Although our final goal is to create a system which requires no human intervention, the assistance of human expert in this process seems the best solution at present. It is much easier to remove false positive nuclei with this tool than to create a cell lineage from 4D microscope images only by hand.

3.3 Identifying the Same Nuclei Appearing in Different Focal Planes and Time-points

A nucleus may be detected through different focal planes and time-points (See Fig. 7). All such nuclei derived from a single one have to be identified and merged.

Our algorithm first picks up a nucleus at the earliest time-point, and successively searches for its successors. The *nearest* nucleus which is detected on the same focal plane at the next time-point is regarded as the successor. By the word *nearest*, we mean that the 2D Euclidean distance between the centroids of the nuclei is the smallest. If the distance to the successor is greater than a certain threshold, the successor is discarded and this procedure is carried on for another nucleus.

Next, our algorithm searches for a nucleus detected on consecutive focal planes at the same time-point by a similar procedure.

Finally, our algorithm weaves together the results described above. Every pair of sets consisting of nuclei recognized to be derived from a single nucleus are joined into one set if there exists a nucleus which is a member of the both sets. The procedure continues until all such pairs are joined.

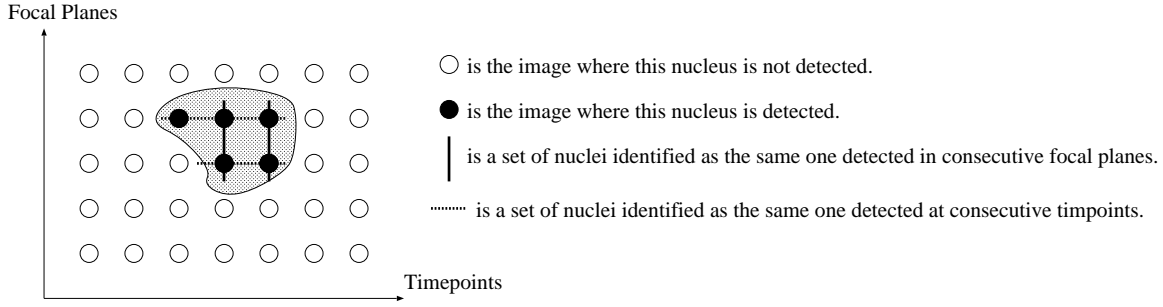


Figure 7: A nuclei detected through different focal planes and time-points. All such nuclei derived from a single one have to be identified.

From the information of this algorithm, we can find out where and when a nuclei emerged and disappeared.

3.4 Cell Lineage Construction

This section describes the algorithm which constructs a hypothetical cell lineage based on the nucleic information created with the algorithm presented in Section 3.3. Although the true cell lineage can be represented as a single tree structure, the 4D microscope images might have, in general, multiple nuclei at the earliest time-point. Therefore our algorithm creates as many lineage trees as nuclei at the earliest time-point.

Our algorithm searches for all nuclei whose starting time-point is the first time-point of the data set. For each such nucleus n_r , an initial lineage tree which consists of only a root nucleus n_r is created.

Then, our algorithm repeats the following procedure.

Let n_p be a nucleus, whose disappearing time-point is the earliest among the nuclei already in some current lineage tree, and whose daughter cells were not searched for. Now our algorithm searches the daughter cells of n_p .

Among the nuclei not yet added to any of current lineage trees, our algorithm repeatedly searches for two nuclei n_1 , n_2 whose emerging points are the first nearest and the second nearest to the disappearing point of the nuclei n_p . If the distance between n_1 and n_p is less than a threshold given *a priori*, n_1 is regarded as a daughter cell of a parent cell n_p and n_1 is added to the current cell lineage. The same goes for n_2 .

This repetition goes on while any of the cell lineages continues to grow. The distance between centroids of two nuclei is measured by 4D Euclidean distance with weights for time-point axis C_t and for focal-plane axis C_z , as follows.

$$d = \sqrt{(x_1 - x_2)^2 + (y_1 - y_2)^2 + (C_z(z_1 - z_2))^2 + (C_t(t_1 - t_2))^2}$$

Here, (x_1, y_1, z_1, t_1) , (x_2, y_2, z_2, t_2) are the positions of centroids of two nuclei.

4 Computational Experiment

4.1 Parameters for the Algorithm

In this section, we briefly show the parameters used by our system.

4.1.1 Parameters for Size Constraints

Here we give parameters used when we choose nuclei etc. from connected component of pixels in binarized output of filters. They are: i) the minimum covering area S_{\min} , ii) the maximum covering area S_{\max} , iii) the minimum outline length l_{\min} , iv) the maximum outline length l_{\max} , v) the minimum roundness r_{\min} , and vi) the maximum roundness r_{\max} .

	S_{\min}	S_{\max}	l_{\min}	l_{\max}	r_{\min}	r_{\max}
Detector A	150	1300	40	200	3	1
Detector B	170	1300	50	140	0.7	1
Detector C	30	350	0	100	0.5	1
Boundary Detector	150	500	150	200	0	0.5
Egg-Area Detector	0	$+\infty$	0	$+\infty$	0	1

4.1.2 Parameters Specific to Each Algorithm

To determine the values of some of the parameters described below, we performed a number of computational experiments varying the parameters and adopted the best one.

For Detector A, The range of smoothing $m = 30$, the threshold when the result is binarized $T = 155$. For Detector B, The threshold when the result is binarized $T = 160$, the threshold applied to the output Prewitt operator $T' = 115$. For Detector C, The direction along which the calculation is performed $\theta = 0.43\pi$. The range where the calculation performed $m = 30$. The threshold when the result is binarized $T = 155$. For Boundary Detector, The threshold applied to the output Prewitt operator $T = 115$. For Egg-Area Detector, The threshold applied to the output Kirsch operator $T = 115$.

4.1.3 Same Nucleus Identifier

The maximum distance between centroid of two regions which is recognized as the same region, $M = 130$.

4.1.4 Cell Lineage Construction

The weight for the distance over focal plane, $C_z = 3$. The weight for time-point axis, $C_t = 10$. The maximum distance between the disappearing point of a parent cell and the emerging point of a daughter cell, $C_d = 100$.

4.2 Accuracy of Our Nuclei Detector.

To measure the accuracy of our nuclei detector, we applied the detector to the following 17 microscope images which were selected by an expert.

$$\begin{aligned}
 &I_{01,30}, I_{01,42}, I_{02,40}, I_{03,40}, I_{06,35}, I_{08,32}, \\
 &I_{08,38}, I_{10,40}, I_{10,50}, I_{12,33}, I_{12,40}, I_{15,24}, \\
 &I_{15,40}, I_{15,45}, I_{17,23}, I_{20,29}, I_{20,40}
 \end{aligned}$$

The result is summarized in Table 1. In this paper, we refer to a nucleus by the name of the cell [8] containing the nucleus. For example, by the notation ‘AB’, we refer to the nucleus of the AB cell.

There were 46 nuclei detected by a human expert, and 33 of them were detected by our system. Out of the 13 nuclei which our system could not detect, 7 nuclei were detected on a different focal plane at the same time-point, 4 nuclei were on their way of division and did not appear clearly in the images, and 2 nuclei were in a dark area of the images and seemed somewhat hard to be detected. 7 false positives (regions which are not actually nuclei) also came out as outputs.

Table 1: The result of the nucleus detector.

Time point	Focal plane	Nuclei detected by a human expert	Nuclei detected by our system	Comment on the nucleus not detected.
01	30	AB,P ₁	AB,P ₁	
01	42	AB,P ₁	AB,P ₁	
02	40	AB,P ₁	AB,P ₁	
03	40	AB,P ₁	AB,P ₁	
06	35	ABp	ABp	
08	32	ABa,ABp	ABa,ABp	
08	38	ABa,ABp,P ₂ ,EMS	ABa	ABp was detected in $I_{8,33}$. P ₂ was detected in $I_{9,36}$. EMS was detected in $I_{10,40}$. P ₂ was detected in $I_{10,34}$.
10	40	ABa,ABp,P ₂ ,EMS	ABa,ABp,EMS	
10	50	ABa,ABp	ABa,ABp	
12	33	ABa,ABp,P ₂ ,EMS	ABa,ABp,P ₂	EMS was detected in $I_{12,38}$.
12	40	ABa,ABp,P ₂ ,EMS	ABa,ABp,EMS	P ₂ was detected in $I_{12,38}$.
15	24	ABpr,ABar,P ₂	P ₂	ABpr was detected in $I_{18,23}$. ABar was detected in $I_{15,29}$.
15	40	P ₂	P ₂	
15	45	P ₂ ,ABpl	P ₂	ABpl was detected in $I_{16,47}$.
17	23	P ₂ ,ABpr,ABar	P ₂	ABpr was detected in $I_{18,23}$. ABar was detected in $I_{15,29}$.
20	29	ABal,ABar,MS	ABal,MS	
20	40	ABal,ABpl,E	ABal,ABpl,E	ABar was detected in $I_{20,32}$.
-	-	46 nuclei	33 nuclei	

4.3 Hypothetical Cell Lineage Constructed by Our System

This section describes the hypothetical cell lineage which our system constructed.

4.3.1 The Output of the Nuclei Detector

Our nuclei detector was executed on the 4D microscope image of *C.elegans* embryo described in Section 2. A human expert examined this image and detected 12 nuclei of the following cells: AB, ABa, ABal, ABar, ABp, ABpl, ABpr, P₁, EMS, P₂, E, and MS [8].

First, we used the algorithm described in Section 3.3 without the removal of false positives. We show the results in Table 2. Only part of the result is shown because the result contained 259 nuclei², and it is not realistic to show them all.

Table 2: A sample of detected nuclei.

ID	# of images	emerging point	disappearing point
ID000	17	(08:259,101,00)	(10:256,091,03)
ID001	1	(17:198,282,00)	(17:198,282,00)
ID002	1	(19:115,224,01)	(19:115,224,01)
ID003	1	(06:169,249,02)	(06:169,249,02)
ID004	1	(04:270,077,03)	(04:270,077,03)
ID005	1	(19:113,222,03)	(19:113,222,03)
ID006	4	(06:169,253,05)	(06:169,253,05)
ID007	1	(00:114,213,05)	(00:114,213,05)
ID008	1	(13:158,150,05)	(13:158,150,05)
ID009	1	(04:115,223,07)	(04:115,223,07)
ID010	3	(08:256,101,08)	(08:256,101,08)

4.3.2 The Output of the Nuclei Detector Refined by a Human Expert

There is a very large number of false positives included in the 259 detected nuclei, and we cannot expect our system to construct an accurate hypothetical cell lineage with these many false positives. By using the GUI tool described in Section 3.2, this problem may be overcome.

Falsely detected nuclei may appear in any of the 1780 images. A human expert of our laboratory examined all of these images. It took about three hours for him to remove all of the false positives, which is roughly 6 seconds per image. The number of nuclei extracted from this refined data was 52,

²This is a terribly large number. Remember that there are only 12 nuclei in the data set.

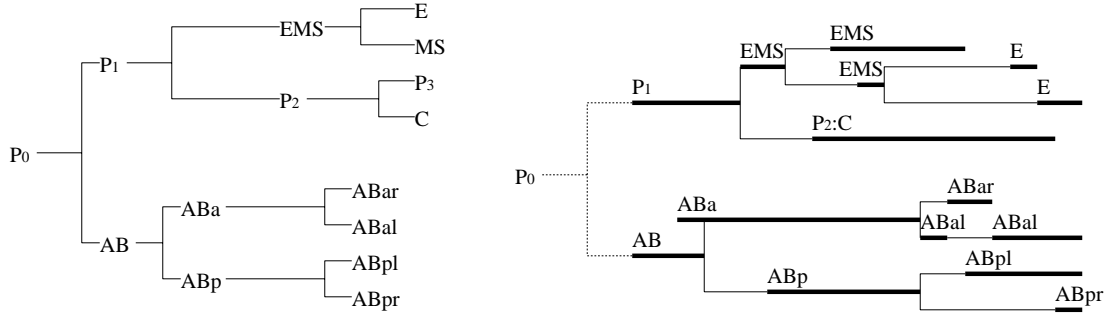


Figure 8: The left tree is the true cell lineage [8]. Here, forking points show the time-points of cell division. The right tree is the cell lineage constructed by our system. Here, each thick line represents a detected nucleus. Each end of the thick line represents the time-point when the corresponding nucleus emerges or disappears. P₂ and C was recognized as a single nucleus, written as P₂:C in this figure.

still larger than the true number 12. This is due to the fact that our algorithm sometimes fails to connect the nuclei derived from a single nucleus.

Among these 52 nuclei detected, 24 were nuclei detected in only one image, 8 in only two images, and 5 in only three images. We presumed that nuclei detected in less than 5 images were fragments of some nucleus, and constructed a hypothetical cell lineage based only on nuclei detected in 5 images or more. The number of such nuclei used for the cell lineage was 15.

4.3.3 Hypothetical Cell Lineage

The hypothetical cell lineage constructed by our system is shown in Fig. 8. This is consistent with the true cell lineage up to 6-cell stage except that P₂ was joined to C and ABal, EMS, and E are multiply detected falsely. Instead of these errors in nucleus detection, the topology of this tree is fairly consistent to the true cell lineage. Our cell-lineage constructing algorithm seems robust against multiple detection of a single nucleus.

5 Conclusion and Future Work

5.1 Conclusion

We have developed a system that automatically constructs a cell lineage from 4D Nomarski DIC images, and have succeeded in constructing a cell lineage of *C. elegans* close to the true lineage, up to the 7-cell stage. Also, a GUI tool was developed in order to get rid of falsely identified nuclei before beginning to construct the cell lineage. The usefulness of the tool has been verified.

5.2 Future Work

Nucleus Detector In order to construct a reliable hypothetical cell lineage, It is important to improve the accuracy of the nuclei detector: higher sensitivity and less false positives.

More knowledge on the appearance of a nucleus could be utilized to predict where a nucleus should exist or not. The result of detection at different time-point or on different focal plain may also be used. A more sophisticated method to integrate the three nuclei detector may also improve the accuracy.

Cell Lineage Constructor It should be a promising approach to establish the problem of constructing the cell lineage as an optimization problem. This can be done by constructing a function that calculates the “goodness” of a hypothetical cell lineage.

With this approach, we can easily implement a new condition for a better cell lineage by just modifying the objective function.

Our 4D Nomarski DIC Microscope System Although it is important to construct a cell lineage of *C. elegans* embryo later than 7-cell stage, the data set we used consists of the 4D images of *C. elegans* from 2-cell stage up to 7-cell stage.

We are now setting a 4D Nomarski DIC microscope system in our laboratory that allows us to acquire 4D images of *C. elegans* as we want. Using this system, we will be able to examine the availability of our cell lineage algorithm on 8-cell stage or later.

Our image processing algorithm does not work well when applied to a 2D image of embryo later than 10-cell stage. More sophisticated image processing algorithm will be required.

Acknowledgments

We thank Dr. Asako Sugimoto and the Yamamoto Laboratory of the Department of Bio-chemistry, University of Tokyo, who kindly gave us an opportunity to take images of the *C. elegans* embryo with a Nomarski DIC microscope. We also thank Dr. Yuji Kohara at National Institute of Genetics, Mishima, Japan. The original idea of this project was formed in the discussion with him.

References

- [1] Horvitz, H.R., Genetics of Cell Lineage, in *The Nematode Caenorhabditis elegans*, ed. by Wood, W.B., Cold Spring Harbor Laboratory, 1988.
- [2] Hutter, H. and Schnabel R., *glp-1* and inductions establishing embryonic axes in *C. elegans*, *Development*, 120:2051–2064, 1994.
- [3] Jähne, B., Haußecker, H., and Geißler, P., *Handbook of Computer Vision And Applications Volume 2: Signal Processing and Pattern Recognition*, Academic Press, 1999.
- [4] Kirsch, R., Computer determination of the constituent structure of biological images, *Comput. Biomed. Res.*, 4:315–328, 1971.
- [5] Prewitt, J.M.S., Object enhancement and extraction, in *Picture Processing and Psychopictorics*, Academic Press, New York, 75–149, 1979.
- [6] Schnabel, R., Hutter, H., Moerman, D., and Schnabel, H., Assessing normal embryogenesis in *Caenorhabditis elegans* using a 4D microscope: variability of development and regional specification, *Developmental Biology*, 184:234–264, 1997.
- [7] Spector, D.L., Goldman, R.D., and Leinwand, L.A., *Cells - A Laboratory Manual, Volume 2: Light Microscopy and Cell Structure*, Cold Spring Harbor Laboratory Press, 1998.
- [8] Sulston, J.E., Schierenberg, E., White, J.G., and Thomson, J.N., The embryonic cell lineage of the nematode *Caenorhabditis elegans*, *Developmental Biology*, 100:64–119, 1983.
- [9] Takagi, M. and Shimoda, H., *Handbook of Image Analysis*, University of Tokyo Press, 1991. (In Japanese)